Available online at www.sciencedirect.com
SCIENCE DIRECT
Polymer 46 (2005) 2141–2152
polymer
www.elsevier.com/locate/polymer

Amphiphilic poly(acrylic acid-*b*-styrene-*b*-isobutylene-*b*-styrene-*b*-acrylic acid) pentablock copolymers from a combination of quasiliving carbocationic and atom transfer radical polymerization

R.F. Storey*, A.D. Scheuer, B.C. Achord

Department of Polymer Science, School of Polymers and High Performance Materials, The University of Southern Mississippi, P.O. box 10076, PSRC 305, Hattiesburg, MS 39406, USA

Received 21 September 2004; received in revised form 10 December 2004; accepted 13 December 2004
Available online 29 January 2005

Abstract

Amphiphilic poly(acrylic acid-*b*-styrene-*b*-isobutylene-*b*-styrene-*b*-acrylic acid) (PAA-PS-PIB-PS-PAA) block copolymers were prepared using a combination of quasiliving carbocationic and atom transfer radical polymerization (ATRP) techniques. Poly(styrene-*b*-isobutylene-*b*-styrene) (PS-PIB-PS) block copolymer macroinitiators with targeted molecular weights and high degrees of chain end functionality ($F_n > 1.7$) were prepared by quasiliving carbocationic polymerization of isobutylene followed by sequential addition of styrene. Poly(*tert*-butyl acrylate-*b*-styrene-*b*-isobutylene-*b*-styrene-*b*-*tert*-butyl acrylate) (PtBA-PS-PIB-PS-PtBA) pentablock terpolymers with targeted molecular weights and low polydispersities (PDIs) were synthesized from the PS-PIB-PS macroinitiators via ATRP of tBA using either a Cu(I)Cl/1,1,4,7,7-pentamethyldiethylenetriamine (PMDETA) or Cu(I)Cl/tris[2-(dimethylamino)ethyl]amine (Me_6TREN) catalyst system. Deprotection of the *tert*-butyl groups using trifluoroacetic acid at 25 °C resulted in the formation of PAA-PS-PIB-PS-PAA pentablock terpolymers. Comonomer composition of the final terpolymers, determined by ^{1}H-NMR spectroscopy, was very close to theoretical.

Keywords: Polyisobutylene; Block copolymers; Atom transfer radical polymerization

1. Introduction

Recent advancements in 'living'/controlled polymerizations such as group transfer [1], carbocationic, [2,3] ring-opening, [4,5] and free-radical polymerizations [6–9] have dramatically increased the variety of macromolecular architectures and topologies that can be synthesized. The synthesis of block copolymers (BCPs) with predictable molecular weights, narrow molecular weight distributions (MWDs), and terminal functionalities typically requires a 'living'/controlled polymerization technique. These polymerizations are characterized by an equilibrium between an inactive (dormant) and active species, in which the latter exists in a concentration many orders of magnitude lower than the former. Termination of these polymerizations results in predictable chain-end functionalities based upon the dormant species, which is necessary for the synthesis of well-defined block copolymers.

Atom transfer radical polymerization (ATRP) is a reversible redox process, typically between halogenated chain ends and a complexed copper halide species (i.e. Cu(I)Cl or Cu(I)Br), which can be used to yield well-defined (co)polymers. Using an alkyl halide initiating species, such as benzyl bromide or chloride, various acrylates, methacrylates, and styrenics have been polymerized in a controlled manner (i.e. targeted molecular weights and MWDs < 1.5) employing this polymerization technique. While the range of monomers that can be polymerized using ATRP has increased over the past several years, polymerization of

* Corresponding author. Tel.: +1 6012664879.
E-mail address: robson.storey@usm.edu (R.F. Storey).

0032-3861/$ - see front matter © 2005 Elsevier Ltd. All rights reserved.
doi:10.1016/j.polymer.2004.12.041

(meth)acrylic acids and low-reactivity monomers including alkyl-substituted olefins has proven unsuccessful. The polymerization of acrylic acid (AA) using ATRP is unsuccessful because the acid groups in AA can both coordinate to the transition metal and protonate the nitrogen-containing ATRP ligands, causing a deactivation of the ATRP polymerization. The problem with ATPRP of monomers inherently low reactivity is difficulty of activation of the halogenated chain end, leading to an impractically low radical concentration.

Quasiliving carbocationic polymerization (QCP) is applicable to monomers such as isobutylene (IB) and styrene and yields, among other interesting structures, poly(styrene-*b*-isobutylene-*b*-styrene) (PS-PIB-PS) triblock copolymers [10–12] with predictable molecular weights, narrow MWDs, and well-defined block junctions. The synthetic utility of QCP is limited by the relatively narrow range of monomers to which it can be applied. Since the reactive site is a carbocation, electrophilic monomers such as (meth)acrylates cannot be polymerized by this technique.

Combination of 'living'/controlled polymerization techniques enables the creation of copolymers that otherwise cannot be synthesized. In theory, block copolymers synthesized by two different polymerization techniques are possible if the first polymer block contains or can be functionalized with a group that is an efficient initiator for the subsequent polymerization technique. This general process has been termed site transformation. Many polymerization techniques including condensation (step growth) [13], anionic [14], ring-opening [15], and especially cationic [16–24] processes have been combined with ATRP to yield novel polymer structures that were previously unattainable.

The combination of QCP and ATRP to form PIB-based block copolymers is of specific interest to this work. ATRP of a wide variety of styrenic and (meth)acrylate monomers has been demonstrated using chemically modified PIB macroinitiators [17–19]. In several cases, PIB modification involved the quantitative transformation of the PIB *tert*-chloride chain ends to bromoisobutyrate (–OCOC$(CH_3)_2$Br). This was carried out by conversion of allyl-terminated linear or star PIB homopolymer to primary alcohol-terminated PIB by a hydroboration-oxidation reaction and subsequent reaction with 2-bromo-2-methylpropionyl bromide to yield bromoisobutyrate-terminated PIB. This macroinitiator effectively polymerized 2-(dimethylamino)ethyl methacrylate [17], *tert*-butyl methacrylate [18], and acrylonitrile [19]. Hydrolysis of the *tert*-butyl groups formed poly(isobutylene-*b*-methacrylic acid), an amphiphilic linear block copolymer [18]. While this method is effective, multiple synthetic steps are required to create the PIB-based macroinitiator.

A grafting-from technique has also been used to create branched copolymers from a PIB-based macroinitiator. Commercially available poly(isobutylene-*co*-*p*-methylstyrene-*co*-*p*-bromomethylstyrene) (EXXPRO®) was used as a macroinitiator for the ATRP of styrene [20,21] and methyl methacrylate (MMA) [21]. The mechanical properties of the final copolymers varied from an elastomer to a toughened glassy polymer when the weight fraction of the side chains was either low or high, respectively. In addition, DSC and DMA showed the presence of two glass transition temperatures, suggesting phase separated behavior, which was confirmed by SAXS measurements. In a variation of the above approach, poly[(*p*-bromomethylstyrene-*co*-*p*-methylstyrene)-*b*-isobutylene-*b*-(*p*-bromomethyl-styrene-*co*-*p*-methylstyrene)] was prepared using QCP and subsequently used as a macroinitiator in conjunction with a Cu(I)Br/bipyridine catalyst system for the ATRP of styrene and *p*-acetoxystyrene [22]. The ATRP polymerizations were only taken to ~15% monomer conversion; nonetheless, homopolymer impurities due to thermal initiation of the monomer were formed, as evidenced by the presence of a low molecular peak in the SEC traces.

Another method that is particularly relevant to this study involves the in situ end-capping of quasiliving PIB with styrene resulting in *sec*-benzyl chloride chain termini that are capable of initiating ATRP [16,23,24]. It was demonstrated that only a small number (3–6) of styrene units is necessary for successful site transformation. A-B-A triblock copolymers containing PIB center blocks and outer blocks from monomers such as styrene [23,24], *p*-acetoxystyrene [24], methyl acrylate (MA) [23], MMA [23] and isobornyl methacrylate [23] were synthesized via ATRP using these PIB macroinitiators.

In this paper, we have used a method similar to that above, except that the styrene content was increased to form a pentablock structure. The general synthesis is outlined in Scheme 1 and first involves the synthesis of PS-PIB-PS BCPs via sequential quasiliving cationic polymerizations of isobutylene and styrene from a difunctional initiator. The resulting macroinitiators are subsequently used under ATRP conditions to initiate the controlled polymerization of tBA yielding PtBA-PS-PIB-PS-PtBA pentablock terpolymers (PTPs). Deprotection of the *tert*-butyl groups results in the formation of well-defined, amphiphilic PAA-PS-PIB-PS-PAA PTPs. Copolymers that incorporate IB and AA are experimentally attractive because IB is highly non-polar and has high thermal and oxidative stability while AA imparts hydrophilicity and adds a site for further modification. These studies form a synthetic foundation for the creation of novel, multiphasic thermoplastic elastomers containing hydrophobic (PIB and PS) and hydrophilic (PAA) block segments.

2. Experimental

2.1. Materials

The preparation of 5-*tert*-butyl-1,3-bis(2-chloro-2-propyl)benzene (*t*-Bu-*m*-DCC) has been previously reported [25]. Isobutylene (IB) and CH_3Cl (MeCl) (both BOC Gases,

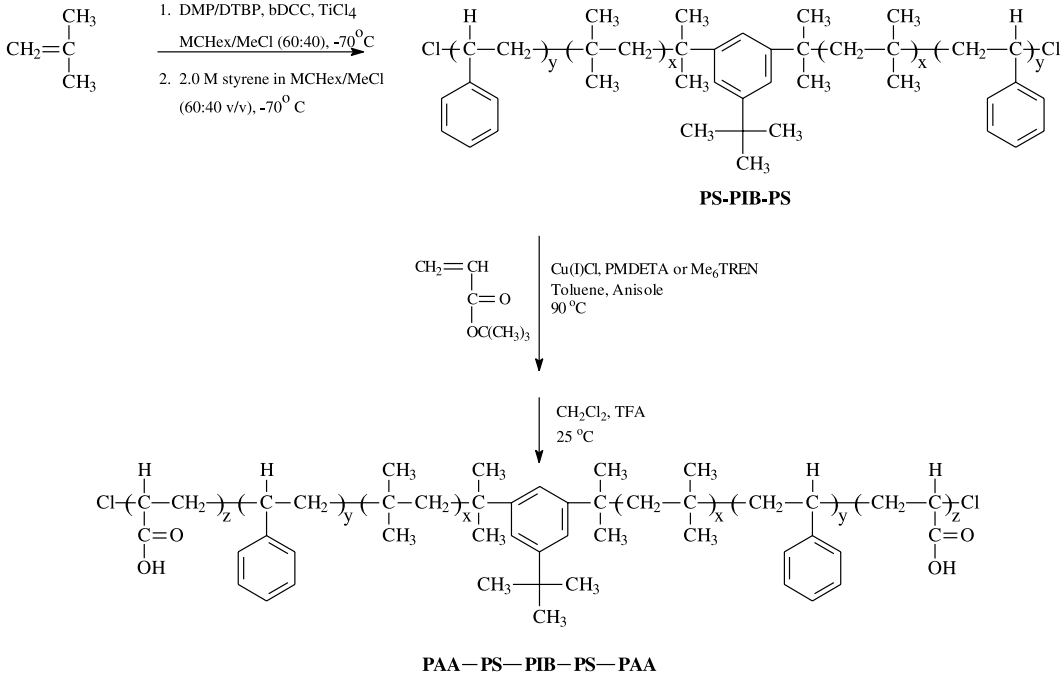

Scheme 1.

99.5%) were dried through columns packed with $CaSO_4$ and $CaSO_4$/4 Å molecular sieves, respectively. Styrene (99%), *tert*-butyl acrylate (tBA, 98%), and 2,6-di-*tert*-butyl pyridine (DTBP, 97%) were all purchased from Sigma-Aldrich Corp. and distilled from CaH_2 under reduced pressure. Cu(I)Cl (99+%, purified), $TiCl_4$ (99.9%, packaged under N_2 in SureSeal bottles), 2,6-dimethylpyridine (DMP, 99+%), anhydrous methylcyclohexane (MCHex, 99+%), anhydrous methanol (MeOH, 99.8%), anisole (99%), trifluoroacetic acid (TFA, 99%), formaldehyde (37 wt% solution in water), formic acid (95–97%), tris(2-aminoethyl)amine (96%), DOWEX®MSC-1 macroporous ion-exchange resin (Dowex sodium, strong cation, 20–50 mesh), and aluminum oxide (alumina, standard grade, activated, neutral, Brockmann I, ~150 mesh, 58 Å) were all used as received from Sigma-Aldrich Corp. 1,1,4,7,7-Pentamethyldiethylenetriamine (PMDETA) (99%) and toluene (anhydrous, 99.8%), both from Sigma-Aldrich Corp. were deoxygenated by sparging with dry $N_{2(g)}$ for 30 min before use. Tris[2-(dimethylamino)ethyl] amine (Me_6TREN) was synthesized using a modification of a previously reported procedure [26].

2.2. Instrumentation

2.2.1. Size exclusion chromatography

Molecular weights and polydispersities (PDIs) of polymers were determined using a SEC system consisting of a Waters Alliance 2690 Separations Module, an on-line multiangle laser light scattering (MALLS) detector (Mini-DAWN™, Wyatt Technology Inc.) and an interferometric refractometer (Optilab DSP™, Wyatt Technology Inc.), as previously described [11]. Freshly distilled THF served as the mobile phase and was delivered at a flow rate of 1.0 ml/min. Sample concentrations were 5 mg/ml in freshly distilled THF, and the injection volume was 100 μl.

2.2.2. NMR and FT-IR spectroscopy

Solution ^{1}H-NMR spectra were obtained on a Varian Unity 300 MHz spectrometer using 5 mm o.d. tubes with sample concentrations of 5–7% (w/v), in deuterated chloroform ($CDCl_3$) (Sigma-Aldrich Corp.) containing 0.03% (v/v) tetramethylsilane as an internal reference. ^{13}C-NMR spectra were obtained using sample concentrations of 20% (w/v), in deuterated tetrahydrofuran (*d*-THF) (Sigma-Aldrich Corp.) containing 0.03% (v/v) tetramethylsilane as an internal reference. FT-IR spectra were obtained using a Bruker Equinox 55 FT-IR spectrometer using 32 scans at 4 cm^{-1} resolution. Polymer samples were cast onto a NaCl plate from either CH_2Cl_2 or THF.

2.2.3. Real-time FT-IR ATR spectroscopy

A ReactIR 1000 reaction analysis system (light conduit type) (ASI Applied Systems, Millersville, MD), equipped with a DiComp (diamond composite) insertion probe, a general-purpose type PR-11 platinum resistance thermometer, and CN76000 series temperature controller (Omega Engineering, Stamford, CT), was used to collect spectra of the polymerization components and monitor reactor temperature in real time as previously described [11]. The light conduit and probe were contained within a glove box (MBraun Labmaster 130), equipped with a hexane/heptane cold bath.

2.2.4. Differential scanning calorimetry

Thermal transitions of BCPs and PTPs were studied using a Mettler-Toledo thermal analysis workstation equipped with a model 822e DSC module. Cooling and heating scans of samples weighing 10–16 mg were run over the temperature range (−100)–150 °C at a rate of 10 °C/min under a constant $N_{2(g)}$ flow of 20 ml/min. Data analysis was performed using Star e2/2 software, and glass-transition (T_g) values were taken as the temperature corresponding to well-defined minima in the first derivative curves, i.e., transition mid-point.

2.3. Synthesis of PS-PIB-PS ATRP macroinitiators

The following is a representative procedure for the synthesis of the PS-PB-PS BCPs. The DiComp probe was inserted into a 1000 ml 4-necked round bottom flask equipped with the temperature probe and a stirring shaft with a Teflon paddle. The reactor was placed into the heptane/hexanes bath and allowed to equilibrate to −70 °C. Into the flask were charged 374 ml MCHex (−70 °C), 0.875 g (3.05×10^{-3} mol) *t*-Bu-*m*-DCC, 250 ml MeCl (−70 ° C), 16 μl (7.1×10^{-4} mol) DTBP, and 24 μl (2.1×10^{-3} mol) DMP. This mixture was allowed to stir for 15 min, after which a background spectrum was collected. Once the background spectrum was obtained, baseline spectra were collected after which 64 ml (8.0×10^{-1} mol) IB (−70 °C) was added to the flask. Several monomer baseline spectra were obtained and 2.25 ml (2.05×10^{-2} mol) $TiCl_4$ (neat and at room temperature) was injected into the flask. Once the IB conversion was >99% (t=148 min), a 1–2 ml aliquot was removed from the reaction vessel and added to 10 ml of prechilled MeOH. The molar concentrations of the reaction components were as follows: $[IB]_0=1.2$ M, $[t\text{-Bu-}m\text{-DCC}]_0=4.4\times10^{-3}$ M, $[2,6\text{-DTBP}]_0=1.0\times10^{-3}$ M, $[DMP]_0=3.0\times10^{-3}$ M, and $[TiCl_4]_0=3.0\times10^{-2}$ M (M_n=15,500 g/mol PDI=1.06).

After the consumption of IB, the instrument was reset to monitor the disappearance of styrene (907 cm^{-1}) and several baseline spectra were collected. After this, a prechilled (−70 °C) solution of 43 ml (3.8×10^{-1} mol) styrene in 88 ml MCHex and 76 ml MeCl was added to the reactor. When the styrene conversion reached ~50%, 50 ml prechilled MeOH was added to the reactor. The polymer was precipitated into a 10× volume excess of MeOH and dried in a vacuum oven at 25 °C. The molar concentration of styrene in the addition and in the total reaction was 1.8 and 4.2×10^{-1} M (M_n=23,600 g/mol PDI=1.10).

2.4. Synthesis of PtBA-PS-PIB-PS-PtBA pentablock copolymers by ATRP

Into a ground-glass Kjeldahl style Schlenk flask equipped with a stir bar and a vacuum adapter were charged 35.0 g (1.48×10^{-3} mol) PS-PIB-PS (M_n=23,600 g/mol PDI=1.10), 0.147 g (1.48×10^{-3} mol) Cu(I)Cl, 70 ml toluene, 1.4 ml anisole, 43 ml (2.9×10^{-1} mol) tBA, and 0.31 ml (1.5×10^{-3} mol) PMDETA. The reactor was chilled with $N_{2(l)}$; evacuated, and thawed. This freeze-pump-thaw cycle was repeated a total of three times to remove O_2. An initial aliquot (0.1 ml, t=0 min.) was removed from the reactor via a $N_{2(g)}$ purged syringe, after which the reactor was placed into an oil bath heated at 90 °C. Additional aliquots (0.1 ml) for monomer conversion and kinetic analysis were removed at predetermined times via a $N_{2(g)}$ purged syringe. At a predetermined time, the reactor was immersed into $N_{2(l)}$ to quench the polymerization, and 15 ml CH_2Cl_2 was added to dissolve the polymer. The Cu catalyst was removed by stirring the polymer solution with an excess of DOWEX MSC-1 followed by filtering the solution through neutral alumina. The polymer was obtained by precipitation into a mixture of methanol and water (60:40 v/v) and was dried under vacuum at 25 °C for several days (M_n=42,600 g/mol, PDI=1.23).

Monomer conversion for all polymerizations was determined by ^{1}H-NMR using anisole as an internal standard. Integration of the methoxy resonance in anisole (3.75 ppm) and the vinyl resonance in tBA (5.75–5.60 ppm) at predetermined time intervals allowed for the quantitative determination of tBA conversion. The aliquots were subsequently passed through a column of neutral alumina, vacuum dried at 60 °C, and analyzed by GPC.

2.5. Cleavage of tert-butyl ester side chains

Into a 1000 ml round bottom flask equipped with a magnetic stirrer, 50.0 g (1.17×10^{-3} mol) PtBA-PS-PIB-PS-PtBA (M_n=42,600 g/mol, PDI=1.23, 0.174 mol tBA repeat units) and 500 ml CH_2Cl_2 were added. Upon dissolution of the polymer, 67 ml (8.7×10^{-1} mol) TFA was added, and the reaction was allowed to stir for 24 h at 25 °C. The final polymer was vacuum stripped to remove solvent and TFA, washed overnight with excess deionized water, and dried under vacuum at 25 °C for several days.

3. Results and discussion

3.1. Synthesis of PS-PIB-PS BCPs

ATRP macroinitiators containing a PIB center block and PS outer blocks were prepared using a difunctional cumyl-type initiator (*t*-Bu-*m*-DCC) and $TiCl_4$ coinitiator at −70 °C in a MCHex/MeCl (60/40 v/v) solvent system with DMP and DTBP as Lewis base additives. At >99% conversion of IB, a 2 M charge of styrene in MCHex/MeCl was added, and after ~50% styrene conversion, the polymerization was quenched with cold methanol. Quasi-living carbocationic polymerizations of styrene are not as living as those of IB; thus styrene polymerizations were limited to 50% conversion or less to minimize the occurrence of chain transfer and maximize the *sec*-benzyl

chain end functionality. Under these conditions, chain transfer typically takes the form of electrophilic aromatic substitution involving the terminal carbenium ion and a phenyl ring on the same chain (intramolecular backbiting) or on a different chain (coupling). SEC analysis of the triblock copolymers indicated that there were no high molecular weight peaks indicative of coupling due to the intermolecular EAS reaction, and the triblock copolymers had M_n close to the theoretical value and low PDIs (Table 1).

3.2. PS-PIB-PS BCP End-group functionality

It was necessary to quantify the number average chain-end functionality (F_n) of the PS-PIB-PS BCPs to ensure the preparation of well-defined pentablock terpolymers. This was accomplished using a combination of ^{1}H-NMR spectroscopy and SEC. Fig. 1 is a representative ^{1}H-NMR spectrum of a PS-PIB-PS BCP with the expansion of the *sec*-benzyl chloride proton chain end resonance. The F_n of the triblock copolymers with respect to terminal *sec*-chloride groups was calculated using Eq. 1:

$$F_n = \frac{\#\ sec\text{-benzyl chloride protons}}{\text{total \# molecules}} = \frac{5X_{n,St}A_{PhCHCl}}{Ar} \qquad (1)$$

where, Ar is the integrated peak area of the aromatic region (a) from 6.0–8.0 ppm and A_{PhCHCl} is the integrated peak area of the *sec*-benzyl chloride proton (d) centered at 4.3 ppm. $X_{n,St}$ is the average degree of polymerization of an individual PS outer block calculated from SEC data. The F_n with respect to terminal *sec*-benzyl chloride of various PS-PIB-PS BCPs are reported in Table 1. The *sec*-benzyl chloride functionality was two or slightly less than two for all of the PS-PIB-PS BCPs. This suggested that the materials would make suitable macroinitiators for the synthesis of PtBA-PS-PIB-PS-PtBA PTPs with targeted molecular weights based on the ratio of monomer to initiator and monomer conversion.

3.3. Synthesis and characterization of PtBA-PS-PIB-PS-PtBA

tert-Butyl acrylate was polymerized under ATRP conditions at 90 °C under a N_2 atmosphere in toluene using PS-PIB-PS macroinitiators and either a Cu(I)Cl/PMDETA or Cu(I)Cl/Me_6TREN catalyst/ligand system. Aliquots were removed at predetermined intervals for kinetic and SEC analysis. The polymerizations were light green and homogeneous at the beginning, but became heterogeneous and darker green at higher monomer conversions. The heterogeneity in the polymerization medium is due to the formation of the poorly soluble Cu(II). Table 2 summarizes the polymerization results. Well-defined PTPs were synthesized over a wide range of molecular weights, and $M_{n(exp)}$ agreed well with $M_{n(theo)}$. The controlled nature of the polymerizations over a wide range of targeted tBA X_n's was evidenced by the fact that

Table 1
M_n, PDI, and F_n data for various PS-PIB-PS BCPs

Entry	PIB $M_{n,theo}$ (g/mol)	PIB $M_{n,SEC}$ (g/mol)	PDI	PS-PIB-PS $M_{n,theo}$ (g/mol)	PS-PIB-PS $M_{n,SEC}$ (g/mol)	PDI	$X_{n,St}$	Ar:A_{PhCHCl}	F_n
1[a]	5,280	5,540	1.08	10,300	10,400	1.35	47	135:1	1.7
2[a]	10,300	9,870	1.04	15,400	17,200	1.17	70	191:1	1.8
3[b]	5,180	5,510	1.04	10,300	13,300	1.40	75	221:1	1.7
4[b]	14,900	15,800	1.04	19,900	22,900	1.14	68	174:1	2.0
5[b]	14,900	15,500	1.06	19,800	23,600	1.10	78	196:1	2.0
6[b]	24,800	24,200	1.02	35,200	34,500	1.02	99	263:1	1.9

[a] Prepared using DMP:2,6-DTBP = 1:1 (mol:mol).
[b] Prepared using DMP:2,6-DTBP = 3:1 (mol:mol).

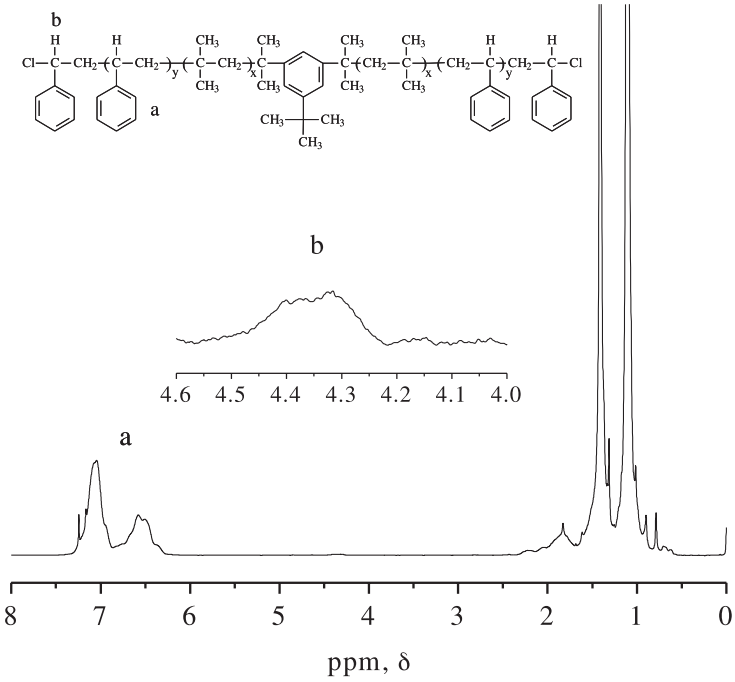

Fig. 1. [1]H-NMR spectrum of PS-PIB-PS with expansion of *sec*-benzyl chloride chain end region (Table 1, entry 5, M_n=23,600, PDI=1.10).

M_n of the PtBA increased linearly with monomer conversion, as shown in Fig. 2. This figure also shows that the polymerization resulted in low PDIs, which was typical for all polymerizations. However, as monomer conversion increased, the PDI increased slightly, suggesting termination activity, which is inherent in free radical polymerizations. Fig. 3 is a representative first-order plot for the ATRP polymerization of tBA using PS-PIB-PS macroinitiators. At higher monomer conversions, deviation from linearity occurred, indicating that the concentration of active species within the polymerization system decreased over time. It is unclear whether this represents a relative increase in the rate of reversible termination (deactivation) or the onset of irreversible termination, or both. The slight increase in PDI with monomer conversion (Fig. 2) suggests irreversible termination, presumably via bimolecular radical–radical coupling; however, the fact that molecular weight continues to increase linearly with monomer conversion suggests that termination is mostly of the reversible type. We hypothesize that the catalyst is deactivated slowly over the course of the polymerization, resulting in an increase in the Cu(II) concentration. This

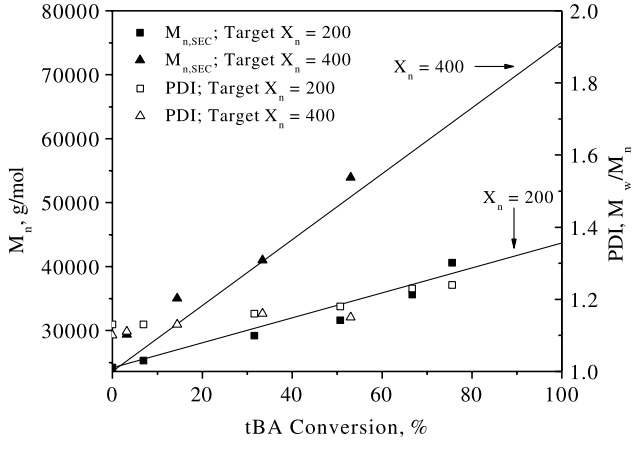

Fig. 2. Plot of M_n and PDI vs conversion for ATRP of tBA using a PS-PIB-PS macroinitiator at 90 °C with differing targeted tBA degrees of polymerization ($X_{n,tBA}$). $X_{n,tBA}=2[tBA]_0/[CE]_0$. Lines are theoretical. $X_{n,tBA}$=200 (Table 2, entry 8): $[tBA]_0$=1.96 M, $[PMDETA]_0$=0.010 M, $[Cu(I)Cl]_0$=0.010 M, $[CE]_0$=0.020 M. $X_{n,tBA}$=400 (Table 2, entry 11): $[tBA]_0$=3.12 M, $[PMDETA]_0$=0.008 M, $[Cu(I)Cl]_0$=0.008 M, $[CE]_0$=0.016 M.

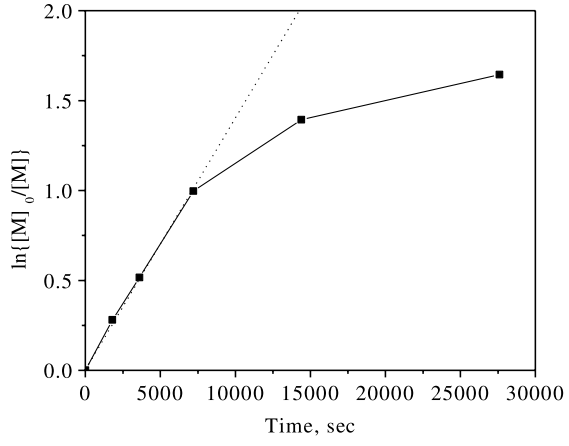

Fig. 3. Plot of $\ln\{[M]_0/[M]\}$ vs time for ATRP of tBA using a PS-PIB-PS macroinitiator in toluene at 90 °C. Dotted line is a visual aid to show linearity at low monomer conversions. PMDETA (0.5:0.5:1) (Table 2, entry 4): $[tBA]_0$=1.42 M, $[PMDETA]_0$=0.011 M, $[Cu(I)Cl]_0$=0.011 M, $[CE]_0$=0.022 M.

Table 2
Results of ATRP of tBA from PS-PIB-PS macroinitiators

Entry	$[tBA]_0$ (mol/l)	$[CE]_0$ (mol/l)	$[Ligand]_0$: $[Cu(I)Cl]_0$: $[CE]_0$	Pzn. Time (min)	Conv. (%)	PS-PIB-PS $M_{n,SEC}$ (g/mol)	PDI	PTP[a] $M_{n,Theo}$[b] (g/mol)	PTP[a] $M_{n,SEC}$ (g/mol)	PDI
1[c]	1.37	0.028	0.5:0.5:1	210	67	10,400	1.35	18,800	20,400	1.32
2[c]	1.44	0.028	0.5:0.5:1	271	87	17,200	1.17	28,500	29,700	1.32
3[c]	1.71	0.034	0.5:0.5:1	140	79	13,300	1.40	23,400	22,000	1.48
4[c]	1.42	0.023	0.5:0.5:1	460	81	23,000	1.14	39,000	38,500	1.31
5[c]	1.56	0.021	0.5:0.5:1	365	76	24,200	1.13	38,700	37,100	1.26
6[d]	1.61	0.021	0.5:0.5:1	240	82	23,600	1.10	39,400	44,300	1.29
7[c]	1.11	0.015	0.5:0.5:1	300	42	34,500	1.08	42,500	40,800	1.13
8[c]	1.96	0.020	0.5:0.5:1	461	75	23,600	1.10	42,700	42,600	1.24
9[c]	2.02	0.020	0.25:0.5:1	240	50	22,900	1.14	35,900	34,500	1.19
10[c]	2.01	0.020	1:0.5:1	240	54	22,900	1.14	36,700	32,900	1.18
11[c]	3.12	0.016	0.5:0.5:1	240	53	23,600	1.14	50,900	53,900	1.15
12[d]	3.10	0.016	0.5:0.5:1	240	71	23,300	1.15	59,400	61,200	1.16
13[c]	2.01	0.020	2:2:1	240	86	22,900	1.14	45,100	45,900	1.30

[a] PtBA-PS-PIB-PS-PtBA.
[b] $M_{n,theo} = 2[tBA]_0 \cdot Conv. \cdot M_{0,tBA}/[CE]_0 + M_{n,SEC\ (PS\text{-}PIB\text{-}PS)}$, $M_{0,tBA} = 128.17$ g/mol.
[c] Ligand: PMDETA.
[d] Ligand: Me_6TREN.

progressively shifts the chain ends toward their dormant state, which is primarily responsible for the observed downward curvature in the first-order plot.

The effect of varying the relative molar amounts of ligand, catalyst, and initiator on the overall rate of polymerization was studied. Fig. 4 compares first-order plots for tBA polymerizations from a PS-PIB-PS macroinitiator, in which the molar concentration of PS-PIB-PS chain ends, [CE], was held constant and the molar concentrations of PMDETA ligand and Cu(I)Cl catalyst were varied. When [catalyst] was held at 0.5 times [CE], all of the plots exhibited a high degree of curvature at short times, and the rate of propagation remained unchanged as [ligand] was varied from 0.5 to 2 times [catalyst]. In contrast, when both [ligand] and [catalyst] were in stoichiometric excess (2:2:1 system), the rate of propagation was significantly higher, and the plot exhibited less curvature. Interestingly, molecular weight increased linearly with conversion for all systems, as shown in Fig. 5.

ATRP polymerizations of tBA were also performed using Me_6TREN as the ligand. Due to its bridged structure [27] and lower redox potential [28], the K_{eq} in ATRP acrylate polymerizations is increased when Me_6TREN is used instead of PMDETA; this was reflected in a higher observed rate of polymerization. Fig. 6 compares the first-order kinetics for the ATRP polymerization of tBA using either PMDETA or Me_6TREN as the ligand. The system that used PMDETA as the complexing ligand at a 0.5:0.5:1 ligand:catalyst:chain end ratio had a $\ln\{[M]_0/[M]\}$ vs time plot that exhibited a high degree of curvature and a slight induction period early in the polymerization. Increasing the

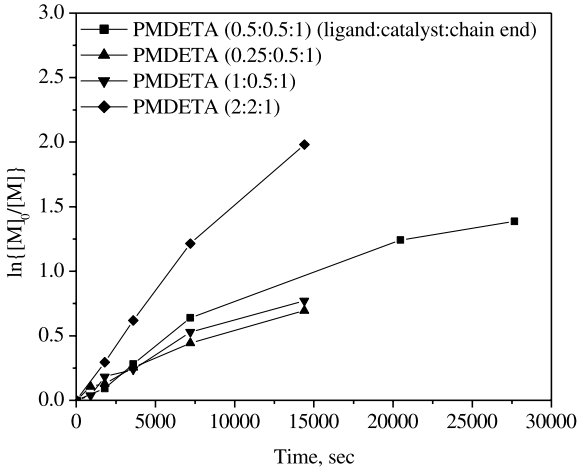

Fig. 4. Plot of $\ln\{[M]_0/[M]\}$ vs time for ATRP of tBA from a PS-PIB-PS macroinitiator in toluene at 90 °C using various molar ratios of ligand:catalyst:chain end. PMDETA (0.5:0.5:1) (Table 2, entry 8): $[tBA]_0 = 1.96$ M, $[PMDETA]_0 = 0.010$ M, $[Cu(I)Cl]_0 = 0.010$ M, $[CE]_0 = 0.020$ M. PMDETA (0.25:0.5:1) (Table 2, entry 9): $[tBA]_0 = 2.02$ M, $[PMDETA]_0 = 0.005$ M, $[Cu(I)Cl]_0 = 0.010$ M, $[CE]_0 = 0.020$ M. PMDETA (1:0.5:1) (Table 2, entry 10): $[tBA]_0 = 2.01$ M, $[PMDETA]_0 = 0.020$ M, $[Cu(I)Cl]_0 = 0.010$ M, $[CE]_0 = 0.020$ M. PMDETA (2:2:1) (Table 2, entry 13): $[tBA]_0 = 2.01$ M, $[PMDETA]_0 = 0.040$ M, $[Cu(I)Cl]_0 = 0.040$ M, $[CE]_0 = 0.020$ M.

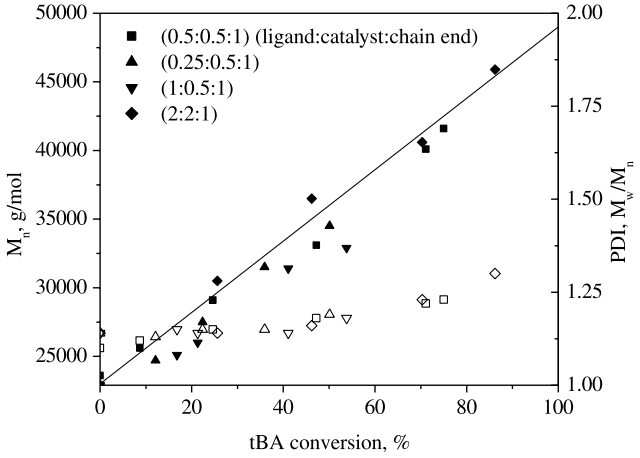

Fig. 5. Plot of M_n and PDI vs conversion for ATRP of tBA from a PS-PIB-PS macroinitiator in toluene at 90 °C using various molar ratios of ligand:catalyst:chain end. PMDETA (0.5:0.5:1) (Table 2, entry 8): $[tBA]_0=1.96$ M, $[PMDETA]_0=0.010$ M, $[Cu(I)Cl]_0=0.010$ M, $[CE]_0=0.020$ M. PMDETA (0.25:0.5:1) (Table 2, entry 9): $[tBA]_0=2.02$ M, $[PMDETA]_0=0.005$ M, $[Cu(I)Cl]_0=0.010$ M, $[CE]_0=0.020$ M. PMDETA (1:0.5:1) (Table 2, entry 10): $[tBA]_0=2.01$ M, $[PMDETA]_0=0.020$ M, $[Cu(I)Cl]_0=0.010$ M, $[CE]_0=0.020$ M. PMDETA (2:2:1) (Table 2, entry 13): $[tBA]_0=2.01$ M, $[PMDETA]_0=0.040$ M, $[Cu(I)Cl]_0=0.040$ M, $[CE]_0=0.020$ M.

ratio of catalyst:ligand:chain end to 2:2:1 caused for a dramatic increase in the rate of polymerization and disappearance of the induction period. The plot for Me_6TREN was similar to that of the 2:2:1 PMDETA system; however, the former plot exhibited a slightly greater deviation from linearity at higher conversions. Control over molecular weight and PDI was unaffected by increasing the amount of catalyst and ligand or changing the identity of the ligand, as illustrated in Fig. 7. The use of Me_6TREN expedites the ATRP of tBA, allowing for the synthesis of high molecular weight PtBA-PS-PIB-PS-PtBA PTPs in a shorter period of time, without sacrificing control of the polymerization.

SEC traces for PS-PIB-PS and PtBA-PS-PIB-PS-PtBA BCPs are illustrated in Fig. 8 and show a clear shift to a lower elution volume after ATRP of tBA. No evidence of unreacted PS-PIB-PS macroinitiator was detected in any of the polymerizations, indicating high initiation efficiency. In addition, all traces were monomodal and showed the absence of PtBA homopolymer impurities.

The structures of the PtBA-PS-PIB-PS-PtBA PTPs were elucidated using ^{1}H-NMR spectroscopy; a representative spectrum is shown in Fig. 9. All of the pentablock BCPs had resonances between 6.0–8.0 (a) and 0.5–2.5 ppm (b), which were associated with the aromatic protons of styrene repeat units and the aliphatic protons from the styrene and IB repeat units, respectively. In addition, the pentablock BCPs contained characteristic peaks associated with PtBA. The methine proton, which is α to the carbonyl group is clearly visible at 2.2 ppm (c). The *tert*-butyl resonances are not observed because they overlap with the *gem*-dimethyl resonances from the PIB centerblock. Additionally, the ultimate methine proton (**d**), adjacent to the chloride end groups is visible at 4.1 ppm. Complete initiation of the PS-PIB-PS macroinitiators is indicated by the absence of the *sec*-benzyl chloride chain end functionality at 4.3 ppm.

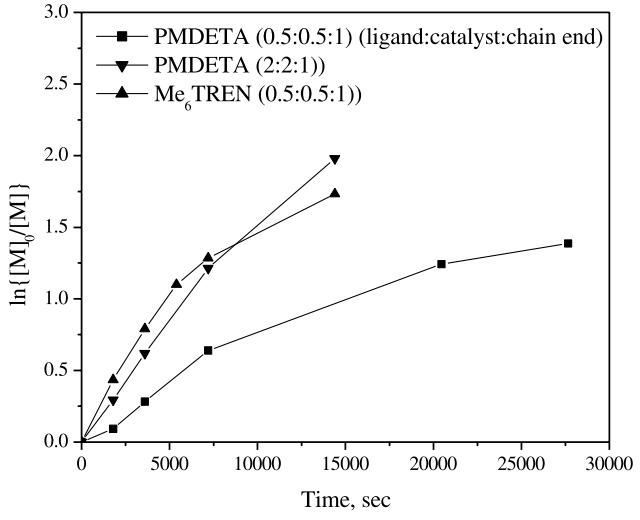

Fig. 6. Plot of $\ln\{[M]_0/[M]\}$ vs time for ATRP of tBA from a PS-PIB-PS macroinitiator in toluene at 90 °C using different ligands. PMDETA (0.5:0.5:1) (Table 2, entry 8): $[tBA]_0=1.96$ M, $[PMDETA]_0=0.010$ M, $[Cu(I)Cl]_0=0.010$ M, $[CE]_0=0.020$ M. PMDETA (2:2:1) (Table 2, entry 13): $[tBA]_0=2.01$ M, $[PMDETA]_0=0.040$ M, $[Cu(I)Cl]_0=0.040$ M, $[CE]_0=0.020$ M. Me_6TREN (0.5:0.5:1) (Table 2, entry 6): $[tBA]_0=1.61$ M, $[Me_6TREN]_0=0.010$ M, $[Cu(I)Cl]_0=0.010$ M, $[CE]_0=0.020$ M.

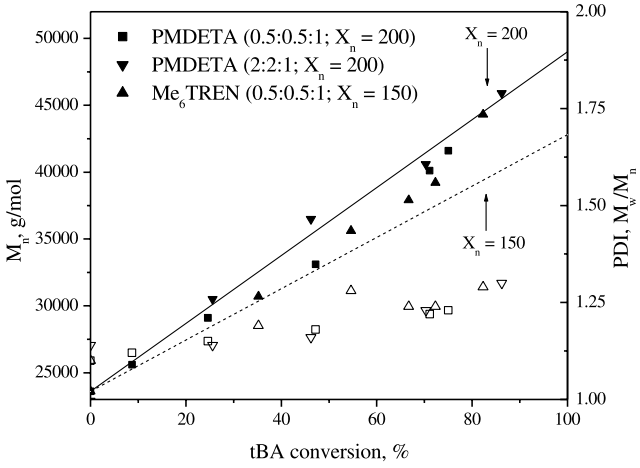

Fig. 7. Plot of M_n and PDI vs conversion for ATRP of tBA from a PS-PIB-PS macroinitiator in toluene at 90 °C using different ligands. $X_{n,tBA}=2[tBA]_0/[CE]_0$. Lines are theoretical. PMDETA, $X_{n,tBA}=200$ (0.5:0.5:1) (Table 2, entry 8): $[tBA]_0=1.96$ M, $[PMDETA]_0=0.010$ M, $[Cu(I)Cl]_0=0.010$ M, $[CE]_0=0.020$ M. PMDETA, $X_{n,tBA}=200$ (2:2:1) (Table 2, entry 13): $[tBA]_0=2.01$ M, $[PMDETA]_0=0.040$ M, $[Cu(I)Cl]_0=0.040$ M, $[CE]_0=0.020$ M. Me_6TREN, $X_{n,tBA}=150$ (0.5:0.5:1) (Table 2, entry 6): $[tBA]_0=1.61$ M, $[Me_6TREN]_0=0.010$ M, $[Cu(I)Cl]_0=0.010$ M, $[CE]_0=0.020$ M.

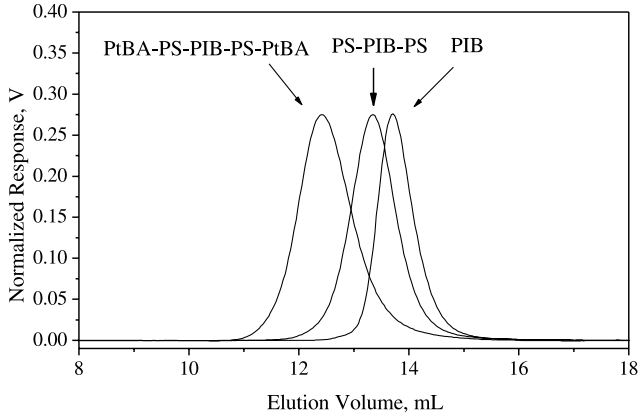

Fig. 8. SEC traces of PIB, PS-PIB-PS, and PtBA-PS-PIB-PS-PtBA (Table 2, entry 10). PIB M_n = 15,800, PDI = 1.03; PS-PIB-PS M_n = 23,300, PDI = 1.15; PtBA-PS-PIB-PS-PtBA M_n = 61,200, PDI = 1.16.

3.4. Synthesis and characterization of PAA-PS-PIB-PS-PAA PTPs

Deprotection of the *tert*-butyl groups in PtBA-PS-PIB-PS-PtBA PTPs was performed at 25 °C for 24 h in CH_2Cl_2 using trifluoroacetic acid (TFA) as the catalyst in a five molar excess relative to the concentration of tBA repeat units. After solvent and catalyst removal, the PAA-PS-PIB-PS-PAA PTPs were washed with excess water and dried at 25 °C under vacuum for several hours. Fig. 10 shows the FTIR spectra of PS-PIB-PS, P*t*BA-PS-PIB-PS-P*t*BA, and PAA-PS-PIB-PS-PAA. In the P*t*BA-PS-PIB-PS-P*t*BA sample, absorbances associated with the tBA functionalities were observed at 1730 and 1150 cm^{-1}, due to the C=O and C–O stretches, respectively. In the deprotected material, the disappearance of the absorbance at 1150 cm^{-1} qualitatively indicated that the *tert*-butyl groups had been successfully removed using TFA. Additionally, carboxylic acid formation was confirmed by the appearance of the characteristic peaks associated with the carboxylic OH and C=O absorbances at 3600–2390 and 1715 cm^{-1}, respectively.

Quantitative deprotection of the *tert*-butyl groups in the PtBA-PS-PIB-PS-PtBA PTPs was elucidated using ^{13}C-NMR spectroscopy. Fig. 11 contains the ^{13}C-NMR spectra of PtBA-PS-PIB-PS-PtBA and PAA-PS-PIB-PS-PAA with expansions of two important regions. Both the protected and deprotected block copolymers contained resonances from the aromatic (a, $CH_2C(H)\mathit{Ph}$, 128 ppm), and methylene (b, $\mathit{C}H_2C(H)Ph$, 61 ppm) carbons of the PS segments and the methylene (b, $\mathit{C}H_2C(CH_3)_2$, 61 ppm), quaternary (c, $CH_2\mathit{C}(CH_3)_2$, 39 ppm), and *gem*-dimethyl (d, $CH_2C(\mathit{C}H_3)_2$, 32 ppm) carbons from the PIB segments. The spectrum of PtBA-PS-PIB-PS-PtBA contains resonances attributed to the carbonyl carbon (e, $CH_2C(H)\mathit{C}OOC(CH_3)_3$, 175 ppm), quaternary carbon in the *tert*-butyl group (f, $CH_2C(H)COO\mathit{C}(CH_3)_3$, 81 ppm), and primary carbons in the methyl *tert*-butyl group (g, $CH_2C(H)COOC(\mathit{C}H_3)_3$, 29 ppm). Close examination of the spectrum for the PAA-PS-PIB-PS-PAA block copolymer reveals that removal of the *tert*-butyl groups was quantitative as evidenced by complete disappearance of the quaternary and primary carbon resonances from the *tert*-butyl groups at 81 and 28 ppm, respectively. Furthermore, the carbonyl

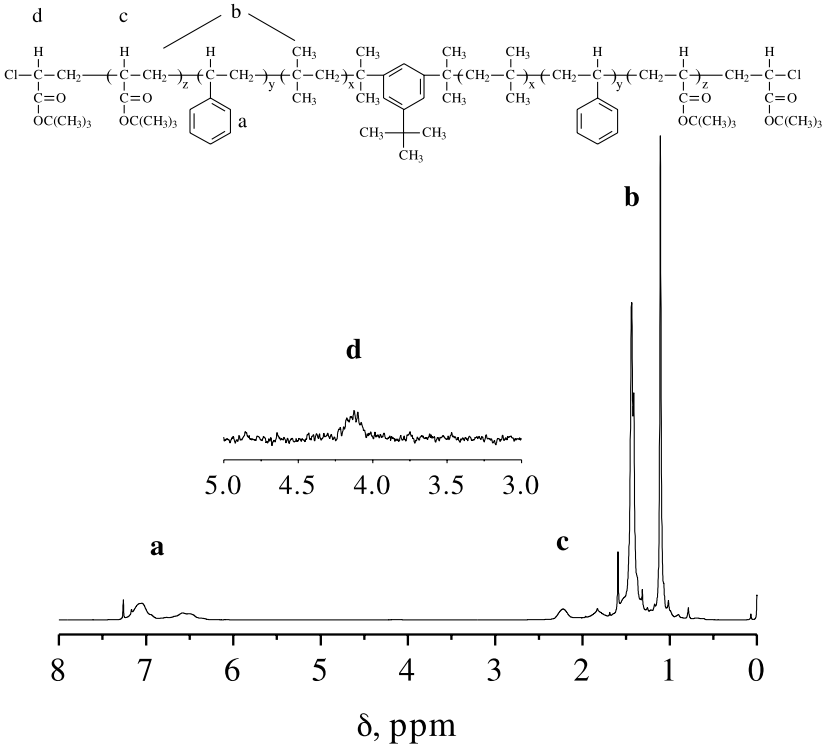

Fig. 9. ^{1}H-NMR spectrum of PtBA-PS-PIB-PS-PtBA with expansion of *sec*- benzyl chloride chain end region (Table 2, entry 2, M_n = 29,700, PDI = 1.32).

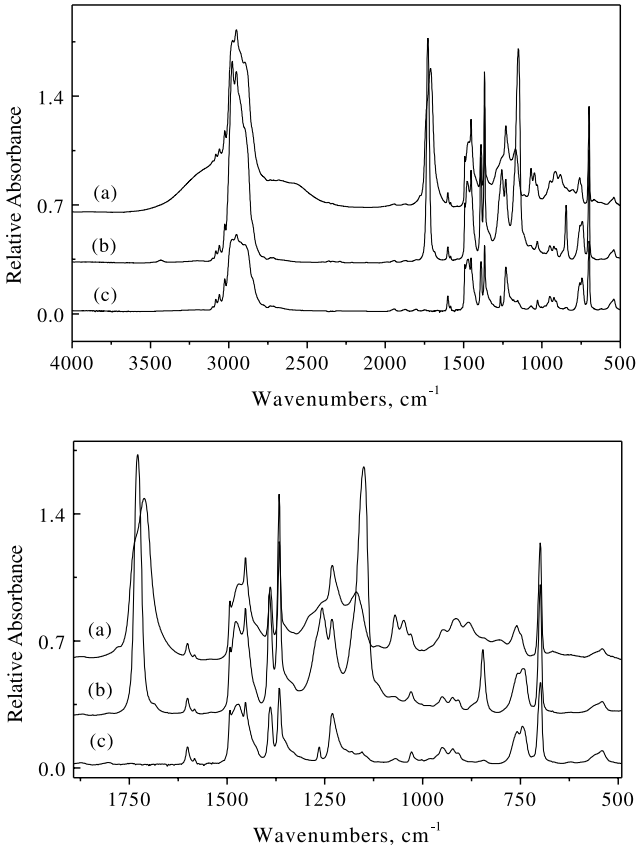

Fig. 10. FT-IR spectra of (a) PAA-PS-PIB-PS-PAA (Table 3, entry 4), (b) PtBA-PS-PIB-PS-PtBA (Table 2, entry 5), and (c) PS-PIB-PS (Table 2, entry 5). Upper: 4000–500 cm^{-1} region. Lower: expansion of 1875–500 cm^{-1} region.

resonance moves downfield from 175 to 177 ppm after deprotection (h, $CH_2C(H)\mathit{C}OOH$, 177 ppm).

Differential scanning calorimetry (DSC) was also used to elucidate the cleavage of the *tert*-butyl ester groups and the phase-separation in the final PTPs. DSC thermograms for PS-PIB-PS, PtBA-PS-PIB-PS-PtBA, and PAA-PS-PIB-PS-PAA are shown in Fig. 12. The glass transition for the PIB phase was observed at −65 °C in all of the samples. After deprotection, the glass transition from PtBA at 47 °C completely disappeared, and a new transition appeared at 125 °C from the poly(acrylic acid) block segments. The unchanged PIB transition and the presence of several distinctive transitions in each sample indicated phase-separation. In addition, the covalent attachment of the acrylic acid segments to the PS-PIB-PS block copolymers did not affect the segmental mobility of the PIB block segment.

3.5. Determination of terpolymer composition

Integrated peak areas of the aromatic and aliphatic regions in the ^{1}H-NMR spectra of PS-PIB-PS triblock copolymers, Ar_t and Al_t, respectively, and PtBA-PS-PIB-PS-PtBA pentablock terpolymers, Ar_p and Al_p, respectively, were used to calculate the comonomer composition of the pentablock terpolymers. The method is based upon the fact that the IB/St repeat unit ratio is the same in both spectra, that is:

$$\frac{N_{IB,t}}{N_{St,t}} = \frac{N_{IB,p}}{N_{St,p}} \tag{2}$$

where, $N_{IB,t}$ and $N_{IB,p}$ are the number of moles of IB repeat units in the triblock copolymer and pentablock terpolymer, respectively, and $N_{St,t}$ and $N_{St,p}$ are the number of moles of styrene repeat units in the triblock copolymer and pentablock terpolymer, respectively. Because Ar_t, Al_t and Ar_p, Al_p were calculated from two separate ^{1}H NMR experiments, the integration values were normalized using the ratio, R_N, of the peak areas for the aromatic regions of the two spectra, as follows:

$$R_N = \frac{Ar_p}{Ar_t} \tag{3}$$

In the triblock copolymer, each styrene repeat unit contributes five protons to Ar_t and three protons to Al_t and each IB repeat unit contributes eight protons to Al_t. Therefore:

$$N_{St,t} = K_t \frac{Ar_t}{5} \tag{4}$$

$$N_{IB,t} = K_t \tfrac{1}{8}\left(Al_t - \tfrac{3}{5}Ar_t\right) \tag{5}$$

where, K_t is the proportionality constant associated with integration of the triblock copolymer spectrum.

In the pentablock terpolymer, the styrene contribution is analogous to Eq. (4):

$$N_{St,p} = K_p \frac{Ar_p}{5} \tag{6}$$

where, K_p is the proportionality constant associated with integration of the pentablock terpolymer spectrum. $N_{IB,p}$ is obtained from the identity in Eq. (2) as follows:

$$N_{IB,p} = N_{IB,t}\tfrac{N_{St,p}}{N_{St,t}} = K_t \tfrac{1}{8}\left(Al_t - \tfrac{3}{5}Ar_t\right)\frac{K_p Ar_p}{K_t Ar_t}$$

$$= K_p \tfrac{1}{8} R_N \left(Al_t - \tfrac{3}{5}Ar_t\right) \tag{7}$$

Each tBA repeat unit contributes 12 protons to Al_p. Therefore, the number of moles of tBA in the pentablock copolymer, $N_{tBA,p}$, is given as follows:

$$N_{tBA,p} = K_p \tfrac{1}{12}\left[Al_p - R_N\left(Al_t - \tfrac{3}{5}Ar_t\right) - \tfrac{3}{5}Ar_p\right] \tag{8}$$

The mole fractions of each type of monomer unit in the pentablock terpolymer may now be calculated directly from Eqs. (6)–(8). Weight fractions of each type of monomer unit, before or after cleavage of the *tert*-butyl side chains, can be calculated using the appropriate repeat unit molecule weights, for example:

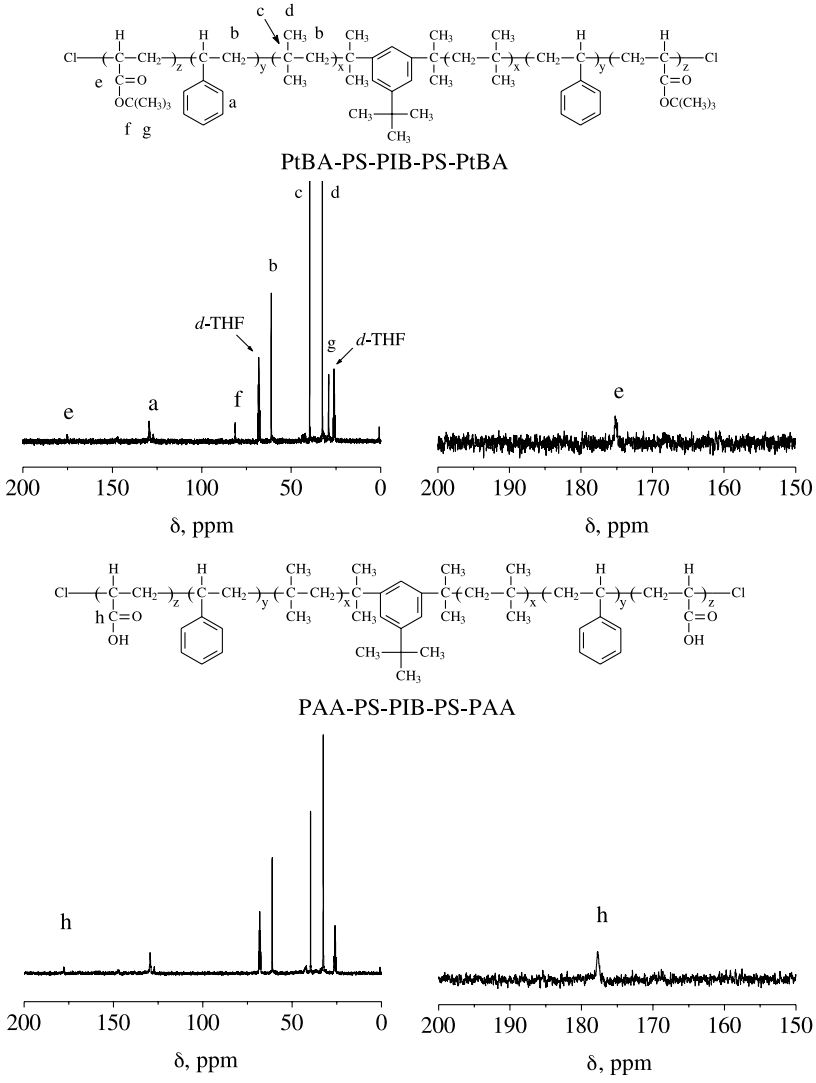

Fig. 11. ^{13}C-NMR of PtBA-PS-PIB-PS-PtBA (Table 2, entry 5) and PAA-PS-PIB-PS-PAA with expansion of carbonyl region.

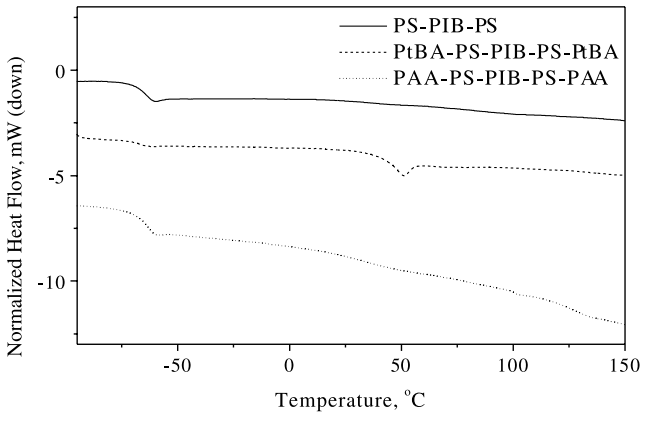

Fig. 12. DSC thermograms of PS-PIB-PS, PtBA-PS-PIB-PS-PtBA, and PAA-PS-PIB-PS-PAA BCPs (Table 2, entry 12).

$$W_{PAA} = \frac{M_{AA}N_{AA,p}}{M_{St}N_{St,p} + M_{IB}N_{IB,p} + M_{AA}N_{AA,p}} \quad (9)$$

where, $N_{AA,p} = N_{tBA,p}$ and M_{AA}, M_{St}, and M_{IB} are the repeat unit molecular weights for acrylic acid, styrene, and IB, respectively.

As shown in Table 3, the experimentally determined terpolymer compositions were very close to the targeted values. These data demonstrate a remarkable degree of synthetic control afforded by these methods with the capability for precise specification of relative block lengths. The latter is very important toward controlling phase-separated morphology, which can have a great effect on the macroscopic properties of the material.

4. Conclusions

Precisely tailored PAA-PS-PIB-PS-PAA PTPs were

Table 3
Comparison of theoretical and experimental compositions of PTPs

Entry	wt% $PS_{(theo)}$	wt% $PS_{(exp)}$	wt% $PIB_{(theo)}$	wt% $PIB_{(exp)}$	wt% $PAA_{(theo)}$	wt% $PAA_{(exp)}$
1	35	33	38	36	27	31
2	30	29	47	44	22	27
3	42	44	33	33	25	23
4	28	27	52	49	20	25
5	27	26	52	51	21	23
6	26	25	51	49	23	26
7	29	29	62	61	9	10
8	25	26	49	51	26	24
9	24	24	56	54	20	22
10	24	24	55	53	21	23
11	23	21	44	40	34	39
12	18	19	35	37	46	44
13	21	20	49	46	30	34

synthesized by a combination of quasiliving carbocationic polymerization and ATRP techniques. The PS-PIB-PS macroinitiators were prepared by quasiliving carbocationic polymerization and possessed a high degree of *sec*-benzyl chloride chain end functionality. Using either a Cu(I)Cl/PMDETA or Cu(I)Cl/Me_6TREN catalyst/ligand system, a variety of PtBA-PS-PIB-PS-PtBA pentablock terpolymers with targeted molecular weights and low PDIs were synthesized from the PS-PIB-PS macroinitiators using ATRP. Cleavage of the *tert*-butyl groups under acidic conditions resulted in the formation of PAA-PS-PIB-PS-PAA PTPs. ^{1}H NMR spectroscopic analysis demonstrated that overall composition and relative block lengths of the terpolymers can be precisely controlled.

Acknowledgements

Support from DEPSCoR (ARO) Grant No. DAAD19-02-1-0155 and the National Science Foundation Materials Research Science and Engineering Center (DMR 0213883) is gratefully acknowledged.

References

[1] Webster OW, Hertler WR, Sogah DY, Farnham WB, RajanBabu TV. J Am Chem Soc 1983;105:5706.
[2] Miyamoto M, Sawamoto M, Higashimura T. Macromolecules 1984; 17:265.
[3] Faust R, Kennedy JP. Polym Bull 1986;15:317.
[4] Endo M, Aida T, Inoue S. Macromolecules 1987;26:2983.
[5] Novak BM, Risse W, Grubbs RH. Adv Polym Sci 1992;102:47.
[6] Georges MK, Veregin RPN, Kazmaier PM, Hamer GK. Macromolecules 1993;26:2987.
[7] Kato M, Kamigaito M, Sawamoto M, Higashimura T. Macromolecules 1995;28:1721.
[8] Wang JS, Matyjaszewski K. J Am Chem Soc 1995;117:5614.
[9] Chiefari J, Chong YKB, Ercole F, Kristina J, Jeffery J, Le TPT, et al. Macromolecules 1998;31:5559.
[10] Kaszas G, Puskas JE, Kennedy JP, Hager WG. J Polym Sci, Part A: Polym Chem 1991;29:427.
[11] Storey RF, Curry CL, Hendry LK. Macromolecules 2001;34:5416.
[12] Gyor M, Fodor Z, Wang HC, Faust R. J Macromol Sci, Pure Appl Chem 1994;A31:2055.
[13] Gaynor SG, Matyjaszewski K. Macromolecules 1997;30:4241.
[14] Hawker CJ, Hedrick JL, Malmstrom EE, Trollsas M, Mecerreyes D, Moineau G, et al. Macromolecules 1998;31:213.
[15] Coca S, Paik HJ, Matyjaszewski K. Macromolecules 1997;30:6513.
[16] Coca S, Matyjaszewski K. Macromolecules 1997;30:2808.
[17] Fang Z, Kennedy JP. J Polym Sci, Part A: Polym Chem 2002;40:3679.
[18] Fang Z, Kennedy JP. J Polym Sci, Part A: Polym Chem 2002;40:3662.
[19] Moustafa AF, Fang Z, Kennedy JP. Polym Bull 2002;48:225.
[20] Fonagy T, Ivan B, Szesztay M. Macromol Rapid Commun 1998;19: 479.
[21] Hong SC, Pakula T, Matyjaszewski K. Macromol Chem Phys 2001; 202:3392.
[22] Truelsen JH, Kops J, Batsberg W. Macromol Rapid Commun 2000; 21:98.
[23] Coca S, Matyjaszewski K. J Polym Sci, Part A: Polym Chem 1997;35: 3595.
[24] Chen X, Ivan B, Kops J, Batsberg W. Macromol Rapid Commun 1998;19:585.
[25] Gyor M, Wang HC, Faust R. J Macromol Sci, Pure Appl Chem 1992; A29:639.
[26] Queffelec J, Gaynor SG, Matyjaszewski K. Macromolecules 2000;33: 8629.
[27] Xia J, Gaynor SG, Matyjaszewski K. Macromolecules 1998;31:5958.
[28] Qui J, Matyjaszewski K, Thouin L, Amatore C. Macromol Chem Phys 2000;201:1625.